Environmental Science & Technology

pubs.acs.org/est

Article

Mobile Measurement System for the Rapid and Cost-Effective Surveillance of Methane and Volatile Organic Compound Emissions from Oil and Gas Production Sites

Xiaochi Zhou, Xiao Peng, Amir Montazeri, Laura E. McHale, Simon Gaßner, David R. Lyon, Azer P. Yalin, and John D. Albertson*

Cite This: *Environ. Sci. Technol.* 2021, 55, 581−592

Read Online

ACCESS | Metrics & More | Article Recommendations | Supporting Information

ABSTRACT: In this study, a ground-based mobile measurement system was developed to provide rapid and cost-effective emission surveillance of both methane (CH_4) and volatile organic compounds (VOCs) from oil and gas (O&G) production sites. After testing in several controlled release experiments, the system was deployed in a field campaign in the Eagle Ford basin, TX. We found fat-tail distributions for both methane and total VOC (C4−C12) emissions (e.g., the top 20% sites ranked according to methane and total VOC (C4−C12) emissions were responsible for ∼60 and ∼80% of total emissions, respectively) and a good correlation between them (Spearman's R = 0.74). This result suggests that emission controls targeting relatively large emitters may help significantly reduce both methane and VOCs in oil and wet gas basins, such as the Eagle Ford. A strong correlation (Spearman's R = 0.84) was found between total VOC (C4−C12) emissions estimated using SUMMA canisters and data reported from a local ambient air monitoring station. This finding suggests that this system has the potential for rapid emission surveillance targeting relatively large emitters, which can help achieve emission reductions for both greenhouse gas (GHG) and air toxics from O&G production well pads in a cost-effective way.

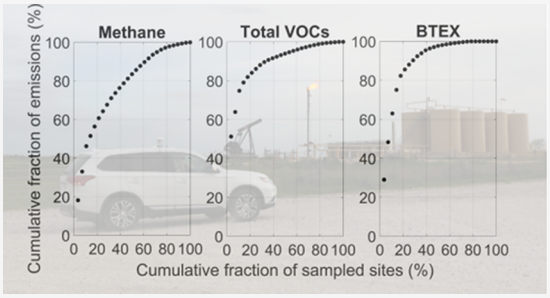

1. INTRODUCTION

Methane is a potent greenhouse gas (GHG) and is the second most prevalent anthropogenic GHG after carbon dioxide.[1] In the United States, the oil and gas (O&G) sector is a large anthropogenic methane emission source, representing 28% of the total methane emissions in 2018.[1] A recent study found that methane emissions from the O&G sector were 60% higher than the United States Environmental Protection Agency (U.S. EPA) GHG inventory estimate, and the greatest discrepancy was in the O&G production segment with a 2-fold difference.[2] Meanwhile, the O&G sector is the largest industrial source of volatile organic compounds (VOCs) in the United States, contributing more than 3 million tons per year according to a 2014 estimate by the U.S. EPA.[3] Some VOCs are hazardous air pollutants (e.g., benzene, toluene, ethylbenzene, and xylene, collectively known as BTEX) and may have direct health impacts for residents nearby O&G production sites.[4−6] VOCs are also precursors of ground-level ozone.[7−9] The U.S. EPA published the New Source Performance Standards (NSPS) in 2016, which included regulations for VOCs and methane from the production and processing segment of the O&G sector.[10] In 2019, the U.S. EPA rescinded the methane requirement in the policy amendment, arguing that regulations for VOCs can simultaneously reduce methane emissions.[11] Some studies have found that methane and VOCs may originate from different sources onsite a O&G production well pad (e.g., separator and storage tank).[12,13] Therefore, the effectiveness of achieving methane and VOC emission reductions by only regulating VOC emissions remains to be examined from additional field measurements. Also, only regulating VOC emissions will be ineffective to reduce methane emissions from dry gas wells.

Considering the presence of the fat-tail distribution for both methane and VOC emissions[13,14] and their spatiotemporal variability of emissions,[15,16] routine emission surveillance that can quickly identify large emitters and prioritize mitigation can be a cost-effective way to achieve efficient overall emission reductions while providing complete coverage of all sites in a region of study. A robust and cost-effective measurement system with a short turnaround time is needed to perform such emission surveillance. Airborne- and ground-based measurement systems have been deployed to study methane and VOC emissions from O&G production well pads. Airplanes equipped with high-sensitivity real-time gas analyzers or imaging spectrometers can measure methane and/or VOC emissions.[17−20] Constrained by

Received: September 28, 2020
Revised: November 20, 2020
Accepted: December 3, 2020
Published: December 14, 2020

https://dx.doi.org/10.1021/acs.est.0c06545
Environ. Sci. Technol. 2021, 55, 581−592

weather conditions and high operational cost, airborne measurements are often limited to deployment in ad hoc field campaigns. Drone-based systems are emerging as a relatively low-cost and rapidly deployable monitoring approach.[21−24] However, their deployment can be limited by payload capacity as well as safety and regulatory-driven constraints on flight paths.

Leak detection and repair (LDAR) surveys following U.S. EPA Method 21[25] or using an optical gas imaging (OGI) camera[26] are ideal for component-level leak detection. However, they cannot provide leak quantification and are very time and resource intensive, thus tending to have infrequent return periods that open the possibility of long-duration problems prior to detection and mitigation. Ground-based mobile measurement systems have shown great potential for identifying and quantifying methane and VOC emissions from O&G production wells.[27−29] Ground-based mobile measurements can host a wide range of equipment (from research grade to low-cost) and provide emission detection and quantification with high spatial resolution. The use of advanced real-time instruments for speciated VOC measurements requires dedicated personnel with specialized training,[12,13,30] which becomes prohibitively expensive to operate routinely. A less expensive system was developed to make *stationary* downwind measurement using an advanced methane analyzer to trigger sampling of VOCs with SUMMA canisters.[29] Such a paired approach relies on favorable wind conditions and is most suited to situations where the methane and VOCs are emitted from the same source, which may not always apply to O&G production wells.[12,13]

This study addresses the development and demonstration of a ground-based mobile measurement system that can perform rapid emission surveillance of both methane and VOCs from O&G well pads. Real-time measurements of methane and total nonspeciated VOCs were made by an advanced methane analyzer and a photoionization detector (PID), respectively. Two methods were proposed to supplement the nonspeciated PID measurements for VOC emission surveillance: one focuses on emission quantification using SUMMA canisters to sample air downwind from the individual well pads, the other one focuses on rapid surveillance of multiple well pads using data obtained from nearby ambient monitoring stations. Bayesian inference was applied to estimate emission rates using repeated downwind plume measurements.[27,31,32] The system was first tested in a series of controlled release experiments and then deployed to measure O&G production well pads in the Eagle Ford basin, TX. The Eagle Ford basin is one of the largest oil fields in the United States; and the state of Texas emitted the largest amount of VOCs among all 50 states according to the 2014 National Emission Inventory.[3] Several studies have quantified regional hydrocarbon emissions from the Eagle Ford basin using monitoring towers or airplane,[33−35] while only a few studies estimated emissions from individual well pads.[29] Elevated ambient BTEX mixing ratios were observed near unconventional O&G production well pads in the Eagle Ford basin; however, BTEX emission rates were not quantified.[36] Here, we present methane and VOC emissions from well pads to test the ability of rapid and cost-effective emission surveillance for both methane and VOCs, to improve our understanding of emissions in this region, and to discuss the implication for reduction strategies for both methane and VOCs.

2. MATERIALS AND METHODS

A mobile measurement system was developed to measure methane and VOC emissions from O&G production well pads using a dedicated methane analyzer and a photoionization detector (PID) supplemented by SUMMA canisters for VOCs. A sport utility vehicle (SUV) was utilized as the mobile measurement platform (MMP), outfitted with a roof-mounted GPS unit (Trimble Geo 7X handheld from Trimble Inc., Sunnyvale, CA) to track its real-time position. The GPS unit samples at 1 Hz frequency, with an accuracy of 5−15 cm for >98% data points after postprocessing.

Two high-precision methane analyzers were used in this study: a research-grade open-path analyzer[37,38] was used in the controlled release experiment and for development of methods, while a commercial close-path analyzer was used in the subsequent field campaign (Picarro G2301 from Picarro Inc., Santa Clara, CA). Both analyzers employ the laser-based cavity ring-down spectroscopy (CRDS) technique, which is a laser absorption method that derives improved sensitivity from a high-finesse optical cavity. The research-grade open-path analyzer has been quantitatively validated against a reference instrument and has been successfully used in the field for hundreds of hours.[38] The commercial Picarro methane analyzer has been successfully deployed in many vehicle-based field studies with robust performance.[31,39−41] A PID was used to measure VOCs at the ppb level (Falco from Ion Science, Cambridge, U.K). PID is nonselective and therefore responds to a broad range of VOCs with different response factors.[42] In this study, a 10.6 eV lamp was used, which is fairly robust and sensitive to many VOCs often found in O&G production sites.[12,39,43] According to the manufacturer, the detector used by Falco (miniPID 2 PPB) has good linearity over its full range (0−50 ppm) and can operate across a wide range of relative humidity conditions (0−99%, noncondensing).[44] However, it is not responsive to ethane and propane, two commonly observed VOCs from O&G productions.

To supplement PID measurements, air samples were taken by 3.2 L SUMMA canisters to provide speciated mixing ratios of VOCs from plumes emitted from the upwind O&G well pads. For each sample, the field technician held the canister steady with its position above and upwind of his/her head and kept the valve open for approximately 1 min.[39] For each sampled site, mixing ratios of 61 nonmethane hydrocarbons (C2−C12) were analyzed from the SUMMA canister by a commercial analytical lab following the EPA's TO-3 method, with a sampling precision within ±5% and a sampling accuracy within ±10%.[45] It should be noted that the reporting limits for C2−C12 VOCs are in the range of 0.5−3 ppb (Supplemental Information B), which are much higher than research grade labs (e.g., 3 ppt).[39,46] Among others, it includes speciated C4−C12 alkanes and C6−C9 aromatics. These VOCs are selected since they are mostly oil and NG production-related compounds. A previous study analyzed 58 nonmethane VOCs (56 of 58 are included in this study) and found that the combined mixing ratio of unknown compounds is <5% of the sum of the 58 nonmethane VOC mixing ratios.[29] Emissions of another two common VOCs, formaldehyde and methanol, have been detected from O&G production well pads.[12,39] However, they are not selected for lab analysis since they are not detectable by the PID using the 10.6 eV lamp. VOC mixing ratios from all of the SUMMA canisters are summarized and included in the Supplemental Information A (Table S1). For rapid emission surveillance, time-averaged VOC data reported by local ambient air monitoring stations using automated gas chromatography (auto-GC) was used when canister data were not available. Due to the difference in sampling strategies, data from the local stations are used to

https://dx.doi.org/10.1021/acs.est.0c06545
Environ. Sci. Technol. 2021, 55, 581−592

understand regional VOC mixing ratios, whereas data from canister samples can better capture emissions from individual well pads. Time synchronization was performed to correct for sampling line delay of the methane analyzer and the PID.

Before the onset of the field campaign, 53 candidate well pads were selected following the criteria that they are less than 150 m upwind of public roads and more than 150 m from other potential emission sources (e.g., other well pads or processing stations) using Google Earth. In addition, we ensured good road access for all of the candidate well pads and scheduled field sampling based on daily metrological and road conditions (e.g., well pads with accessible road on the east side would be sampled with the prevailing wind from west). For each candidate well pad, three downwind mobile passes were first performed with GPS located methane and PID signals recorded. The MMP drove as slow as 5 m/s to capture the spatial structure of the downwind plume.[47] The vehicle was moving almost perpendicular to the prevailing wind direction, which was visually determined by the windsocks installed on the well pads and later confirmed using wind data collected by the sonic anemometer. If elevated methane mixing ratios (>0.2 ppm above background) were detected during the first three passes, the well pad was then identified for further investigation. Out of the 53 candidate well pads, a total of 28 well pads were identified for further study. The identification process is designed to help locate relatively strong sources and to improve the detectability of speciated VOCs collected by the downwind canister samples. However, it certainly excludes candidate well pads with small emissions from further investigation and this must be considered in the statistical interpretations (e.g., sampling roughly the top half of the emitters).

For each of the 28 identified well pads, additional downwind passes (at least 10) were conducted and a representative air sample was taken using a SUMMA canister. Meanwhile, wind speed, wind direction, and air temperature were measured near the identified well pad using a two-dimensional (2D) sonic anemometer (WindSonic 60 from Gill Instruments, Hampshire, U.K.). The sonic anemometer was mounted on a portable meteorological tower (~1.6 m aboveground), which was installed in a relatively flat and open location near the identified well pad. In future applications, one could integrate the sonic anemometer onto the MMP to evaluate wind speed in real time and at the exact sensor location.[48]

2.1. Emission Rate Estimation. A previously developed Bayesian inference approach was adopted to quantify the emission rates of methane and VOCs from the identified well pad.[27,31,32] Following Bayes' theorem, the posterior probability density function (pdf) of the emission rate Q given the observation of C (either measured methane mixing ratio C_{CH_4} or inferred mixing ratio of the ith VOC, C_i) and the ancillary information including the prevailing meteorological conditions (I) is

$$P(Q|C_y, I) = \frac{P(Q|I)P(C_y|Q, I)}{P(C_y|I)} \quad (1)$$

where C_y [ppm × m] is the cross-plume integrated above-ambient mixing ratios. Practically, C_y can be estimated as $C_y = \sum C_a \Delta x$, where C_a is the above-ambient mixing ratios and Δx [m] is the distance between the geo-referenced mixing ratio data points corrected for nonperpendicular angle of traversal. C_a is calculated as: $C_a = C - C_b$, where C is the raw mixing ratios (C_{CH_4} for methane and C_i for VOCs) and C_b is the background mixing ratios. C_b was estimated as the fifth percentile of the ranked time series of $C_{CH_4}(t)$ and $C_i(t)$ for methane and the ith VOC, respectively.[27,28] Real-time methane mixing ratios, $C_{CH_4}(t)$, can be readily measured by the onboard methane analyzer. Time-resolved and speciated VOC mixing ratios can be inferred from fusing the real-time PID readings and the SUMMA canister sample, by assuming that the plume chemical composition remains unchanged during the mobile sampling period (~30 min), and most VOCs contributing to the elevated PID signal were analyzed from the SUMMA canisters

$$\frac{C_i(t)/RF_i}{CP(t)} = \frac{CC_i/RF_i}{\sum_i CC_i/RF_i} \quad (2)$$

where t is the time, $C_i(t)$ is the inferred mixing ratio for the ith VOC, $CP(t)$ is the total nonspeciated VOC mixing ratio reported by the PID, CC_i is the mixing ratio for the ith VOC in the SUMMA canister, and RF_i is the PID's response factor for the ith VOC provided by the manufacturer.[42] RF_i of VOCs are referenced to isobutylene ($RF_i = 1$). The greater the RF_i is, the less sensitive the PID is to the particular VOC.

Assuming that the prior knowledge of Q is limited to its upper and lower bound (Q_{max} and Q_{min}, respectively), a uniform distribution is adopted for ($P(Q|I)$) as a noninformative prior.[31] After the first sensor pass (with a valid measurement of C_y), eq (1) is updated recursively such that $P(Q|I)$ is replaced each time by the posterior pdf $P(Q|c_y,I)$ derived from the previous sensor pass.

$$P(Q|I) = \begin{cases} 1/(Q_{max} - Q_{min}), j = 1 \\ P(Q|C_y, I)_{j-1}, j > 1 \end{cases} \quad (3)$$

where j is a counter for successive sensor passes.

A Gaussian form of the likelihood function is adopted following previous studies[27,31,49]

$$P(C_y|Q, I) = \frac{1}{\sigma_e\sqrt{2\pi}} \exp\left(-\frac{1}{2}\left(\frac{C_y - C_y^M(Q)}{\sigma_e}\right)^2\right) \quad (4)$$

where $C_y^M(Q)$ is the modeled C_y as a function of the candidate emission rate Q. σ_e is the "error scale" that represents a measure of the uncertainty when comparing the modeled $C_y^M(Q)$ against the measurement C_y. The parameterization of σ_e is detailed elsewhere.[31] A simple passive scalar plume model is used for $C_y^M(Q) = Q/\bar{U}D_z$,[27] where $\bar{U}$ is the plume advection speed and D_z represents the plume vertical dispersion. D_z can be estimated using the semianalytical relation[50] $D_z = \frac{A}{\bar{z}} \exp\left[-\left(\frac{Bz}{\bar{z}}\right)^s\right]$, where z [m] is the height of the sensor inlet, $\bar{z}$ [m] is the mean plume height, and A, B, and s are unitless empirical parameters of atmospheric stability and $\bar{z}$.

By updating the prior term $P(Q|I)$ with the posterior ($P(Q|c_y,I)$) derived from the previous sensor pass, $P(Q|c_y,I)$ is calculated recursively to incorporate data collected after each pass and reflect the total weight of the data collected up to that point in time. After the final sensor pass, the estimated leak rate and the associated uncertainty can be estimated by the mode (Q_e) and standard deviation (σ_Q) of $P(Q|c_y,I)$, respectively[31]

https://dx.doi.org/10.1021/acs.est.0c06545
Environ. Sci. Technol. 2021, 55, 581−592

Table 1. Summary of Controlled Release Experiments, Including the Experiment Number (Exp No.), Emission Source, Controlled Emission Rate (Q_0) ± Uncertainty (σ_Q), Mean Downwind Distance (x_m), Number of Downwind Mobile Passes (N_P), Averaged Meteorological Data Reported by Two Nearby Weather Stations, Including the Mean Wind Speed ($\bar{U}$), Mean Wind Direction (θ_m) Clockwise from the North, and the Estimated Emission Rate (Q_e) ± Uncertainty (σ_Q)

exp no.	emission source	controlled emission rate ($Q_0 \pm \sigma_Q$), in scfh	mean downwind distance (x_m), in m	number of downwind passes (N_P)	mean wind speed (U), in m/s	mean wind direction (θ_m), in deg	estimated emission rate ($Q_e \pm \sigma_Q$), in scfh
1	separator prv	18.57 ± 1.79	103.5	10	1.97	131	21.5 ± 4.6
2	separator prv	45.03 ± 4.71	87.4	13	1.51	102	50.1 ± 9.4
3	tank thief hatch	62.53 ± 3.00	87.6	14	1.43	84	61.4 ± 15.4
4	tank thief hatch	78.76 ± 2.53	92.4	15	1.35	73	71.8 ± 14.1

$$Q_e = \text{argmax}(P(Q|C_y, I))$$
$$(\sigma_Q)^2 = \int (Q - Q_{Exp})^2 \times P(Q|C_y, I)dQ \quad (5)$$

where $Q_{Exp} = \int Q \times P(Q|C_y,I)dQ$ is the expectation of the posterior pdf.

The emission rates of VOCs that are not detected by PID but are analyzed in the SUMMA canister air sample can be estimated using a ratio method[29,40]

$$\frac{Q_{e,n}}{\sum_i Q_{e,i}} = \frac{CC_n * MW_n}{\sum_i CC_i * MW_i} \quad (6)$$

where MW is molecular weight and the subscript n denotes the nth VOC that was not detected by PID but was later found from the SUMMA canister sample. Although C2−C12 VOCs were analyzed by the SUMMA canister, C2−C3 were either not sensitive to PID (e.g., acetylene, ethane, and propane) or found to be below detection limit (i.e., propene) from all of the SUMMA canisters. Therefore, eq 6 will only be used to infer C4−C12 VOCs.

Some of the observed well pads are quite complex with pump jacks, separators, dehydrators, storage tanks, and flare stack, while others have much less equipment on site. When multiple O&G-related equipment were present on a well pad, they were geo-located using Google Earth (later confirmed by field notes) and $P(Q|C_y,I)$ were estimated individually. Following Zhou et al.,[47] the probability of emissions was assumed to be equal for each equipment group; the probability of emission rates for the identified well pad can be estimated by integrating the $P(Q|C_y,I)$ over all of the equipment groups.

2.2. Controlled Release Testing. The Methane Emission Technology Evaluation Center (METEC) at Colorado State University (CSU) was purpose-built to represent typical O&G facilities, such as production well pads, gathering facilities, and underground distribution pipelines.[51] On-site equipment is outfitted with gas release point(s) to mimic real-world NG emission scenarios, such as vented emissions (e.g., pneumatic devices) and fugitive emissions (e.g., seals, fittings, flanges, etc.). A central control system manages flowrates at all release points allowing emissions to vary over time to meet the specification of the test. Considering the slow chemical reaction rate of VOCs and methane in ambient temperature and pressure compared to the travel time from source to sensor, both can be considered as conserved passive scalars during the downwind measurement periods (typically <half an hour). Since they follow the same principles of plume transport, we contend that the methodological performance for methane emission can be readily applied to that for VOC emissions.

Meteorological data were obtained from two nearby weather stations (both within 500 m from METEC) operated by the Colorado Agricultural Meteorological network (CoAgMet). More specifically, wind speed and direction were measured by a wind anemometer and a wind vane (Wind Sentry from R.M. Young Company, Traverse City, Michigan). The air temperature was measured by a temperature and relative humidity probe (HMP45C-L from Vaisala, Vantaa, Finland). Both stations report time-averaged meteorological data once every 5 min. To better represent meteorological conditions at METEC, the averaged meteorological data recorded by the two stations are used here.

On August 30, 2017, a series of six controlled release experiments were performed at METEC. Each experiment lasted about 20 min, with emissions from the pressure release valve (prv) of the separator and the thief hatch of the storage tank. Two experiments were excluded due to low wind speed (<1 m/s) and high turbulent intensity (the ratio of wind gust to mean wind speed >2).[32] Consequently, four experiments are available for further analysis, and their experimental conditions are summarized in Table 1.

We first evaluate results obtained from the controlled release experiments. As shown in Table 1, emission rates estimated using the Bayesian inference (Q_e) are fairly close to the controlled emission rate (Q_0), with Q_0 within $Q_e \pm \sigma_Q$ for all four experiments. The percentage error (i.e., $(Q_e - Q_0)/Q_0$) ranged from −8 to 15% with an average of bias of 5%, suggesting a solid model performance. The relatively large uncertainty for Q_e is partly due to the low-resolution wind data (5 min acquisition frequency) that has increased the uncertainty in the plume modeling. The same approach has been tested in multiple controlled release experiments with simplified experimental settings and showed good performance with averaged percentage error <10%.[27,32,47] A recent study showed a good agreement between methane emissions of several fertilizer plants measured by a MMP using the abovementioned Bayesian inference[31] and airborne mass balance approach.[52] Another study found that leaky well pads detected by an OGI camera, which could not quantify emission rates, were all identified by a MMP with emission rates quantified by the Bayesian inference approach.[47] The good agreements between the MMP and other methods (i.e., airborne and OGI camera) in field measurements further improve our confidence in the skills of the Bayesian inference approach.

2.3. Field Campaign. A 1 week field campaign was conducted from March 17 to 24, 2018, to characterize emissions

https://dx.doi.org/10.1021/acs.est.0c06545
Environ. Sci. Technol. 2021, 55, 581−592

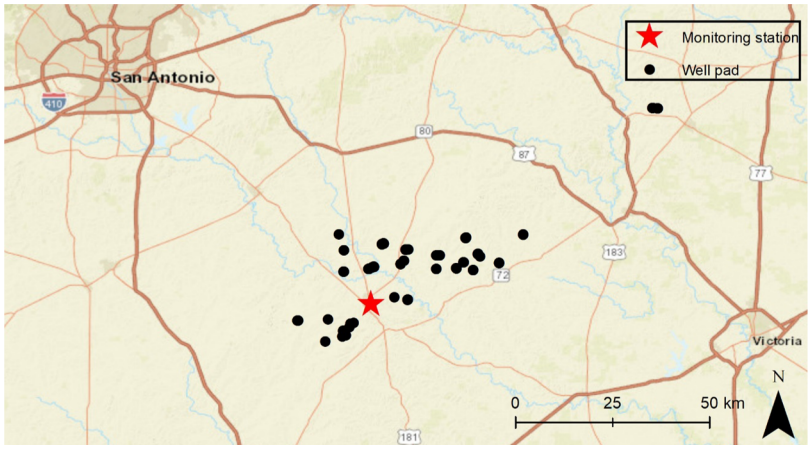

Figure 1. Map of the identified O&G well pads and the local ambient air monitoring station.

Table 2. Summary of Sampled Well-Pad ID, Sampling Date, Time, Mean Downwind Distance (x_m), Number of Downwind Mobile Passes (N_P), Mean Wind Speed ($\bar{U}$), and Mean Wind Direction Clockwise from the North (θ_m)[a]

well-pad ID	date	local standard time	mean downwind distance (x_m), in m	number of downwind passes (N_P)	mean wind speed (U), in m/s	Mean wind direction (θ_m), in deg
1	03/17/2018	12:45−13:21	125	16	2.7	164
2	03/17/2018	14:15−14:44	132	18	3.8	149
3	03/17/2018	14:44−15:13	165	17	3.7	144
4	03/17/2018	15:14−15:42	210	17	3.3	138
5	03/17/2018	16:52−17:27	118	23	3.3	122
6	03/17/2018	17:28−18:02	81	23	4.3	139
7	03/18/2018	15:28−15:45	137	11	2.9	143
8	03/18/2018	16:36−17:04	155	12	3.9	132
9	03/19/2018	10:43−11:15	107	18	4.6	339
10	03/19/2018	11:47−12:16	141	17	2.3	316
11	03/19/2018	14:55−15:20	97	21	3.1	321
12	03/19/2018	16:09−16:32	50	16	2.8	315
13	03/19/2018	16:55−17:20	51	16	2.5	327
14	03/20/2018	12:04−12:43	90	16	2.8	347
15	03/20/2018	12:04−12:43	107	16	2.8	347
16	03/21/2018	11:04−11:33	240	12	3.4	106
17	03/22/2018	10:20−10:44	85	10	4.9	153
18	03/22/2018	10:44−11:07	43	12	4.9	153
19	03/22/2018	13:07−13:57	149	15	4.3	152
20	03/22/2018	16:48−17:18	115	10	6.3	144
21	03/22/2018	16:48−17:18	128	10	6.3	144
22	03/23/2018	10:50−11:19	89	17	5.0	152
23	03/23/2018	12:43−13:03	80	15	4.1	145
24	03/23/2018	15:10−15:38	120	13	4.2	144
25	03/23/2018	17:13−17:46	104	11	5.0	150
26	03/23/2018	17:13−17:46	192	10	5.0	150
27	03/24/2018	07:37−08:00	171	10	1.7	161
28	03/24/2018	08:00−08:23	95	10	2.1	161

[a] x_m, $\bar{U}$, and θ_m are averaged from data collected when sampling each well pad.

of methane and VOCs from active horizontally drilled O&G well pads located in Karnes and DeWitt County, which are part of the Eagle Ford Basin, TX (Figure 1). All of the identified well pads are in open and relatively flat shrubland/grassland. No other known methane and VOC emission sources, such as dairy farms, landfills, or non-O&G stationary combustion sources (e.g., boilers and heaters), were observed during the field campaign. In addition, all measurements were conducted in the absence of upwind mobile combustion sources (e.g., pick-up trucks) to avoid VOC emission interference.

Sampling conditions of the 28 identified active O&G well pads (out of the 53 candidate well pads) are provided in Table 2. No field experiments were excluded due to low wind speed and high turbulent intensity conditions since the mean wind speed ($\bar{U}$) > 1 m/s for all well pads in Table 2. A neutral atmospheric condition was assumed based on climatological analysis of a nearby flux tower, and sensitivity analysis showed that the estimated emission rates were only slighted affected (<5%) by typical variability of atmospheric stability in this region. For future application, measurements of local atmospheric stability

https://dx.doi.org/10.1021/acs.est.0c06545
Environ. Sci. Technol. 2021, 55, 581−592

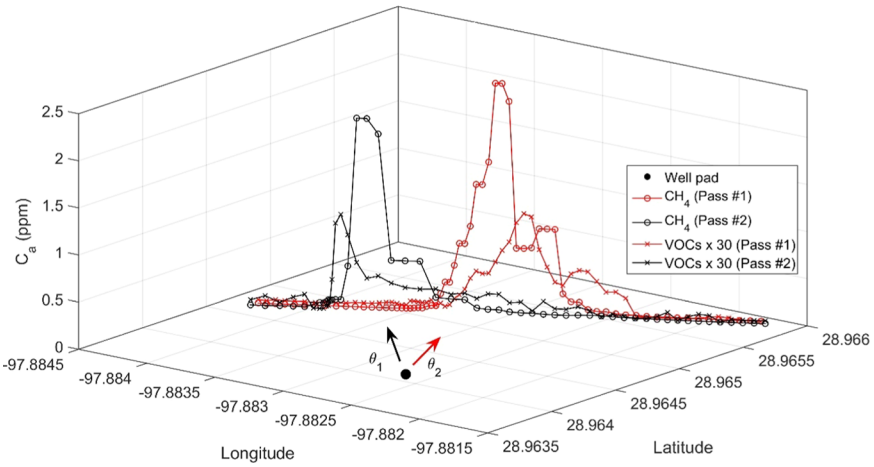

Figure 2. Examples of above-ambient mixing ratios (C_a) for methane and total nonspeciated VOCs measured by the PID (multiplied by a factor of 30 for visual interpretation) at 1 Hz sampling frequency. The vehicle drove from northeast to southwest (left to right on the figure) for Pass #1 at ∼5.3 m/s and from southwest to northeast (right to left on the figure) for Pass #2 at ∼5.7 m/s. Pass #1 and Pass #2 are collected on 03/17/2018, from 12:57:16 to 12:58:22 and from 13:10:20 to 13:11:21, respectively.

(i.e., using a three-dimensional (3D) sonic anemometer) would readily remove this aspect of the uncertainty related to plume dispersion modeling. Sometimes multiple well pads were located along the same road and were sampled sequentially in a single downwind mobile measurement (e.g., well pad #14 and #15 in Table 2). For each well pad, at least one whole air sample was collected using a 3.2 L SUMMA canister downwind from the target well pads. All of the SUMMA canister sample data are included in the Supplemental Information B.

To ensure the sensor performance, three-point calibrations were performed every other day during the field campaign. The isobutylene gas (1 and 10 ppm) was used to calibrate the PID as recommended by the manufacturer.[42] We found consistent and satisfactory performance for the PID and the methane analyzer, with little drift and good accuracy (<8% for PID and <1.5% for methane analyzer at calibration points) during the field campaign. Linear regression curves were established for both sensors (with $R^2 > 0.95$) to postprocess the data.

Ambient VOC data was reported by an auto-GC in a local air monitoring station located in Karnes City, TX, which is within 50 km from most of the identified well pads (Figure 1). Hourly averaged mixing ratios of 46 nonmethane VOCs were measured at the station, 42 out of 46 were also analyzed by the SUMMA canisters, omitting propylene, 1,3-butadiene, isoprene, and *t*-2-butene from the overlap.[53]

3. RESULTS AND DISCUSSION

For C4−C12 VOCs, around 70% (39 out of 56) can be detected by the PID with a measured response factor. The remaining 30% C4−C12 VOCs could not be accurately measured by the PID, and their emissions can only be inferred using canister data (eq 6). It was found that the combined mixing ratio of those nondetectable VOCs was <2% of the total C4−C12 mixing ratio averaged over all canister samples. This result supports the use of PID for VOC (C4−C12) measurements from the well pads in oil and wet gas basins such as the Eagle Ford.

The average background methane mixing ratio found throughout the study was 1.92 ± 0.02 ppm. In March 2018, the monthly average methane mixing ratio at Mauna Loa, Hawaii was 1.87 ± 0.02 ppm. The higher background methane mixing ratio measured in the field is partly caused by the regional enhancement, as found in previous studies.[39] This also applies to the estimated background VOC mixing ratios, which were higher than the measured VOC mixing ratios from the local ambient air monitoring stations. To test the hypothesis that the plume VOC compositions remained relatively unchanged during the mobile sampling period (∼30 min), multiple SUMMA canister samples were taken consecutively downwind from two well pads. It was found that the composition of various VOCs (represented as the percentage of total mixing ratios) sampled from the different canisters were very close (maximum difference <5%), which provides support for the hypothesis. More details about the tests can be found in the Supplemental Information A (Section S2).

3.1. Emission Rate Estimation. We present an example of the measurements made on March 17, 2018 in Figure 2 (Well pad ID #1 from Table 2), showing the above-ambient mixing ratio of methane and total nonspeciated VOCs measured along two downwind passes. The start and end of the driving route were determined such that the measured mixing ratios were close to ambient mixing ratios, as shown in Figure 2. Methane and total nonspeciated VOC plumes were both observed during both passes, though plume centers were not entirely overlapped (i.e., the location of the peak methane and VOC mixing ratios were offset by 3 and 4 s for pass #1 and #2, respectively). We postulated that small offsets may be caused by the difference in response time (e.g., time to reach 90% of the actual mixing ratios or t_{90}) for the methane analyzer (<3 s) and the PID (<10 s). Due to the meandering of the wind (as suggested by the instantaneous wind directions θ_1 and θ_2 for passes 1 and 2, respectively), the plume shifted between passes.

The inferred emission rates for methane and two examples of VOCs (i.e., *i*-butane and toluene) are plotted in Figure 3. The results for all of the detectable VOCs are included in the Supplemental Information A (Section S3). For all three compounds, the posterior pdfs $P(Q|C_y,I)$ tend to "sharpen" with additional downwind passes, from a relatively broad pdf (e.g., the black dash lines representing the pdf after the first pass) to a narrower pdf (e.g., the solid red lines representing pdf after the final pass). Estimation uncertainty, which can be visually interpreted as the width of the pdf, was gradually reduced especially after the first several passes. This result clearly illustrates the capability of the recursive Bayesian inference

https://dx.doi.org/10.1021/acs.est.0c06545
Environ. Sci. Technol. 2021, 55, 581−592

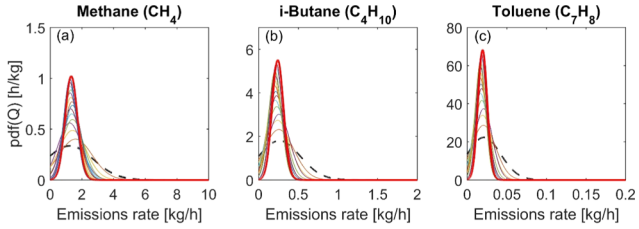

Figure 3. Posterior probability of emission rate Q, $P(Q|C_{yi}I)$, derived from the Bayesian inference for (a) methane, (b) *i*-butane, and (c) toluene. The black dash lines represent the pdf(Q) after the first pass, and the red solid lines are the pdf(Q) after the final pass.

model, which sharpens its lens on the underlying hidden variables as successive measurement passes are obtained.

We compared the emissions estimated using VOC mixing ratios obtained from the SUMMA canisters with those derived from directly adopting the local ambient air monitoring station mixing ratios (Figure 4). The station-based emissions were estimated by replacing the term CC_i (the mixing ratio for the *i*th VOC in the SUMMA canister) in eq 2 with the mixing ratio of the *i*th VOC reported by the local ambient air monitoring station. As expected, the station-based estimates differed somewhat from the canister-based estimates, since the latter fail to capture well pad-specific VOC mixing ratios. The canister-based emission estimates for VOCs will be used in the following analysis, as they certainly reflect more accurate and localized information. Considering the wide range of emissions for total VOCs (C4−C12) and BTEX, their correlations were evaluated using the Spearman's rank correlation coefficient (Spearman's R), which were less affected by the large values. A strong correlation was found between the station-based and canister-based emission estimates for C4−C12 total VOCs (Spearman's R = 0.84), while the correlation becomes weak for BTEX (Spearman's R = 0.69). This result indicates that VOC mixing ratios reported by local ambient air monitoring stations may be useful to identify relatively large VOC emitters, thus enable rapid surveillance for VOC emissions.

3.2. Emission Rate Distributions and Their Correlations. The emissions of methane, total VOCs (C4−C12), and BTEX from the 28 identified well pads are plotted in Figure 5. Due to the fat-tail distributions for the emission rates, both arithmetic and geometric means are reported and their 95% confidence intervals (CIs) are calculated using bootstrapping.[54] Since the arithmetic means are more affected by the large values in the sample, it is generally higher than the geometric means as shown in Figure 5. The overall measured emissions showed variability ranging over several orders of magnitudes. Excluding the three outliers, the methane emissions range from 0.6 to 12.9 kg/h, which is comparable to the methane emissions of 0.4−10 kg/h estimated previously from a small number of well-pad measurements (N = 4) conducted in the Eagle Ford basin.[28] The three outliers (i.e., representing the largest emitters) are well within the measured outliers in other studies ranging from 10 to >300 kg/h, as summarized by Omara et al.[55] The arithmetic mean emissions (95% CI) of methane is 8.6 (5.3−12.9) kg/h, which is higher than the site-level emissions found in other O&G production basins in the United States, except for the Marcellus Basin (~9 kg/h).[55] This is likely caused by the fact that we only sampled the top ~50% of well pads with relatively large emissions (i.e., 28 out of the 53 candidate well pads), while missing well pads would be expected to have much lower emissions.

The total VOC (C4−C12) emissions exhibited the greatest intersite variability (compared to methane and BTEX), ranging from 0.1 to >100 kg/h. The geometric mean (95% CI) of the total VOC (C4−C12) emission is 2.8 (1.6−4.6) kg/h, which is close to the geometric mean emission of total VOCs (C2−C12) in Anadarko, Barnett, and Permian Basin (2.5−10.6 kg/h)[56] but higher than the geometric mean emission of total VOCs (C3−C12) found in the Barnett, Denver-Julesburg, and Pinedale Basins (0.2−0.9 kg/h).[29] Since C2−C3 VOCs are excluded from our analysis, the total VOC (C2−C12) emission is expected to be even higher considering that the averaged mixing ratios of C2−C3 combined is ~60% of the total mixing ratios in canister samples.

The median BTEX emission is estimated to be 0.05 kg/h, which is close to that found in Upper Green River Basin (UGRB) (~0.06 kg/h)[13] and the Barnett Basin (0.05 kg/h).[40] The geometric mean (95% CI) of BTEX emissions is 0.1 (0.03−0.3) kg/h, which is also similar to the geometric mean (95% CI) of 0.05 (0.03−0.08) kg/h from several O&G Basins.[29] In contrast, the arithmetic mean (95% CI) of BTEX emission is 0.4 (0.1−0.6) kg/h, which is much higher than the arithmetic mean

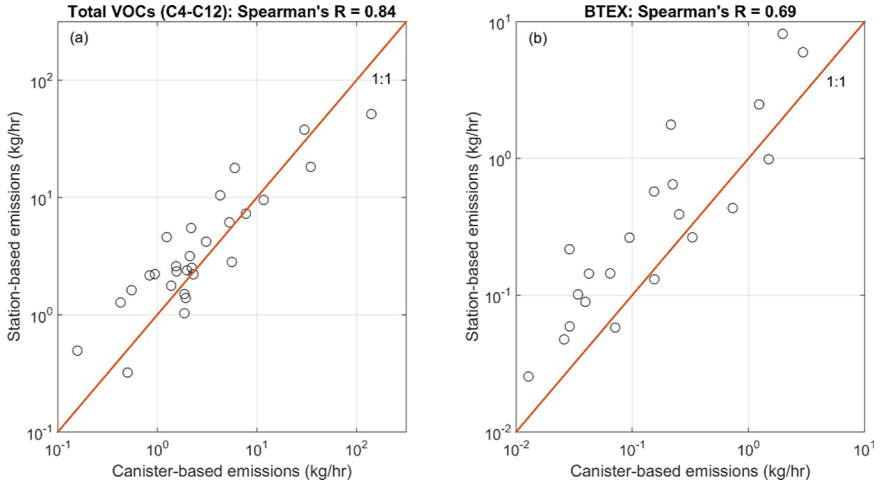

Figure 4. Estimated emission rates using SUMMA canisters and local ambient air monitoring stations for (a) total VOCs (C4−C12) and (b) BTEX. The Spearman's rank correlation coefficients (Spearman's R) are estimated. The red lines are the 1:1 line.

https://dx.doi.org/10.1021/acs.est.0c06545
Environ. Sci. Technol. 2021, 55, 581−592

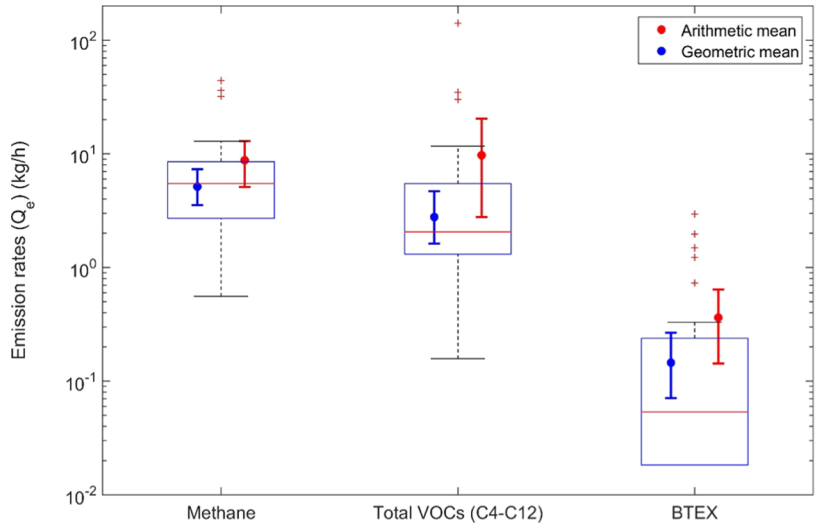

Figure 5. Estimated emission rates (Q_e) for methane, total VOCs (C4−C12), and BTEX across all of the sampled well pads. The results are presented as boxplots, with red lines indicating medians, and the bottom and top edges of the boxes indicating the 25th and 75th percentiles, respectively. The whiskers extend to the most extreme data points not considered as outliers, and the outliers are plotted as red crosses. The arithmetic means and geometric means of Q_e are shown in red and blue along with their 95% CIs, respectively.

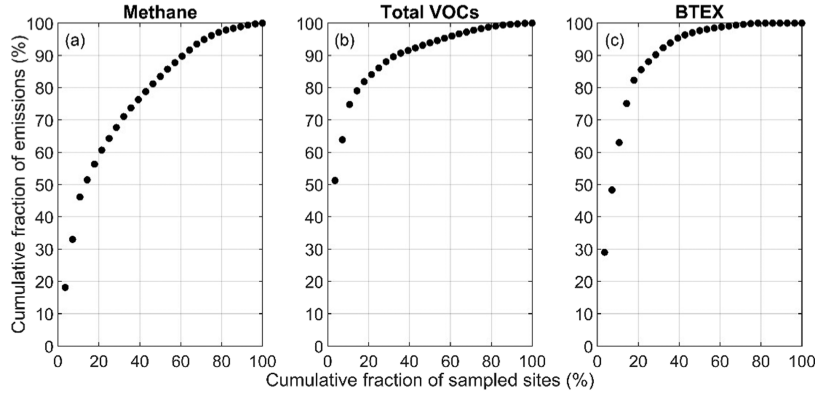

Figure 6. Cumulative fraction of emissions for (a) methane, (b) total VOCs (C4−C12), and (c) BTEX as a function of the cumulative fraction of the sampled well pads (rank ordered).

of 0.09 (0.003−0.38) kg/h found in UGRB.[13] We hypothesize that the great discrepancy is partly caused by the presence of several large BTEX emitters found in this study since we focused on the top ∼50% emitters. Previous work has found that the mean methane emissions (both absolute and production-normalized) were higher in the Eagle Ford Basin than that in the UGRB.[55] It is also possible that the variations between study areas relate to composition oil and gas and the O&G production for those well pads.

The cumulative fraction of total emissions was plotted as a function of the cumulative fraction of the sampled well pads, ranked from large to small emitters (Figure 6). For methane, the top 20% of the total number of sampled well pads were responsible for roughly 60% of total emissions. This is similar to studies in the Barnett and Marcellus basin, where 20% of sources were found to be responsible for 60−90% of emissions.[57,58] A similar pattern is observed for VOCs and BTEX, such that the top 20% of the total number of sampled well pads represented roughly 80% of total emissions. This is slightly more skewed than the observed distribution in the UGRB, where the top 20% of sites were responsible for 67% of BTEX emissions.[13] Again, the fact that this study focused on the top ∼50% emitters would naturally reduce the skewness as compared to an unbiased sampling. More importantly, an overlap was found between large emitters, such that the top 20% well pads ranked according to methane emissions were responsible for 79% of total VOCs (C4−C12), 78% BTEX, and 60% methane emissions. This finding showed that controlling the large emitters (i.e., the top 20%) could be a viable and cost-effective way to achieve emission reductions for both GHG and air toxics (e.g., BTEX) from O&G production well pads.

A good correlation was observed between methane and C4−C12 total VOCs (Spearman's R = 0.74), suggesting that emission controls may help reduce both methane and C4−C12 VOCs in oil and wet gas basin such as the Eagle Ford Basin. Relatively weak correlations were found between BTEX and methane (Spearman's R = 0.47) and between BTEX and total C4−C12 VOCs (Spearman's R = 0.35). We further explored the correlation between BTEX emission and others by introducing the combined C6−C10 VOCs, which are often considered to be gasoline range organics (GRO) or volatile petroleum hydrocarbons (VPH).[59] A correlation of Spearman's R = 0.64 was found between VPH and BTEX, which is superior to the correlations between BTEX and others shown in Table 3. Since VPH are often related to crude oil extraction processes, this

https://dx.doi.org/10.1021/acs.est.0c06545
Environ. Sci. Technol. 2021, 55, 581−592

result indicates that BTEX emissions are likely caused by the oil production and processing on the well pads.

Table 3. Spearman's Rank Correlation Coefficient (Spearman's *R*) between Emissions of Methane, Total VOCs (C4−C12), and BTEX

	methane	total VOCs (C4−C12)	BTEX
methane	1	0.74	0.47
total VOCs (C4−C12)		1	0.35
BTEX			1

3.3. Sensitivity Analysis of Emissions Against Production Data. Well-pad level production statistics were obtained from the national database with data updated for the year 2018.[55] A sensitivity analysis was performed to explore the possible dependence of measured emission rates on daily NG production (in thousands of cubic feet per day or Mcf/d), daily liquid (combined oil and condensate) production (in barrels per day, or bbl/d), and daily produced water (in bbl/d). The results are included in Supplemental Information A (Section 4). Since all of the sampled well pads are fairly new (production age ranges from 0.9 to 8.3 years, with an average of 5.7 years), we do not expect any correlation between the age of well pads and the measured emissions. Little dependences were found between the emissions and production statistics, with all $R^2 < 0.1$. This result is consistent with previous studies[12,28,60] and suggests that a considerable portion of emissions may be fugitive in nature.

4. DISCUSSION

A ground-based mobile measurement system was developed to detect and quantify methane and VOC emissions from O&G well pads using downwind plume measurements. The system was validated in controlled release experiments and successfully deployed to measure methane and VOC emissions from several O&G production well pads in the Eagle Ford basin, TX. A fat-tail distribution was found such that a small fraction of well pads were responsible for most emissions of methane and VOCs. Meanwhile, a good correlation was found between methane and total VOC (C4−C12) emissions (Spearman's $R = 0.74$). More importantly, ∼60% methane emissions and ∼80% VOC and BTEX emissions can be reduced by controlling the top 20% methane emitters. This finding showed that emission surveillance using the proposed mobile measurement system could be a cost-effective way to identify those large emitters and maximize emission reductions for both GHG and air toxics. It should be noted that the well-pad identification process excluded well pads with relatively small emissions from further investigation. Therefore, the measured emissions must be used with caution when attempting to assess regional or basin-wide emissions. Although total VOCs (C4−C12) emission rates estimated using canisters and auto-GC data were somewhat different, a strong correlation was found between them (Spearman's $R = 0.84$), suggesting that the local monitor data can be used for rapid and low-cost surveillance targeting on those large emitters. Such mobile surveillance could be used to trigger a focused follow-up investigation of high emitters with direct measurement techniques, such as an OGI camera, to directly guide repair efforts.

The system has shown a strong ability to detect and quantify emissions from O&G well pads, with the benefit of providing rigorous quantification but noted limitations. First, the measurements were conducted during a relatively short duration, which limited its ability to capture temporal dynamics of emissions as observed in other basins.[14] Second, the success of the mobile sampling approach depends on reasonable road access and favorable meteorological conditions. To improve sampling coverage to remote sites, other methods (e.g., airborne) may be needed to supplement the ground-based approach. Third, the system was tested in a limited number of controlled release experiments during a short duration. A more extensive testing program covering a full spectrum of environmental conditions (e.g., wind speed and temperature) and source complexity (single leak and multiple leak) is needed to fully evaluate the system performance. Fourth, the uncertainties of estimating speciated VOC mixing ratios by fusing the PID data and downwind canister samples were not quantified in this study. Future studies that compare the tracer gas releases or directly measured VOC mixing ratios (e.g., using the proton-transfer-reaction mass spectrometer or PTR-MS) and the PID-derived VOC mixing ratios will be useful to evaluate this uncertainty. Finally, the 10.6 eV lamp equipped with the PID is not sensitive to ethane and propane, two of the major VOCs emitted from the O&G production sites. Other types of methods or analyzers are needed to help quantify emissions of ethane and propane.

■ ASSOCIATED CONTENT

Supporting Information

The Supporting Information is available free of charge at https://pubs.acs.org/doi/10.1021/acs.est.0c06545.

VOCs analyzed in the SUMMA canister, VOC speciation from well pads with multiple SUMMA canister samples, and sensitivity analysis of VOC emissions against production data (PDF)

SUMMA canister data taken downwind from all of the identified well pads (XLSX)

■ AUTHOR INFORMATION

Corresponding Author

John D. Albertson − *School of Civil and Environmental Engineering, Cornell University, Ithaca, New York 14853, United States*; Phone: +1 (607)255-9671; Email: albertson@cornell.edu

Authors

Xiaochi Zhou − *School of Civil and Environmental Engineering, Cornell University, Ithaca, New York 14853, United States*; orcid.org/0000-0002-7123-3835

Xiao Peng − *School of Civil and Environmental Engineering, Cornell University, Ithaca, New York 14853, United States*; orcid.org/0000-0001-9402-2865

Amir Montazeri − *School of Civil and Environmental Engineering and Sibley School of Mechanical and Aerospace Engineering, Cornell University, Ithaca, New York 14853, United States*

Laura E. McHale − *Department of Mechanical Engineering, Colorado State University, Fort Collins, Colorado 80523, United States*

Simon Gaßner − *Department of Mechanical Engineering, Colorado State University, Fort Collins, Colorado 80523, United States*

David R. Lyon − *Environmental Defense Fund, Austin, Texas 78701, United States*; orcid.org/0000-0002-4400-1190

https://dx.doi.org/10.1021/acs.est.0c06545
Environ. Sci. Technol. 2021, 55, 581−592

Azer P. Yalin − *Department of Mechanical Engineering, Colorado State University, Fort Collins, Colorado 80523, United States*

Complete contact information is available at: https://pubs.acs.org/10.1021/acs.est.0c06545

Notes

The authors declare no competing financial interest.

■ ACKNOWLEDGMENTS

We thank Prof. Joe von Fischer from Colorado State University for the use of his Picarro G2301 GHG analyzer for the field campaign. We also thank Beth Trask from Environmental Defense Fund (EDF) San Francisco office to help coordinate the project and the funding, and Mario Bravo from EDF Austin office for help coordinating the field campaign. At Cornell University, the project was supported by the joint research program between EDF and the David R. Atkinson Center for a Sustainable Future (ACSF) at Cornell University, the DOE ARPA-E's Methane Observation Networks with Innovative Technology to Obtain Reductions (MONITOR) program under grant DE-AR0000749. At Colorado State University, the project was supported by an Advanced Industry grant from the Colorado Office of Economic Development and International Trade (award: POGG1 2016-0949).

■ REFERENCES

(1) United State Environemtal Protection Agency. Inventory of U.S. Greenhouse Gas Emissions and Sinks: 1990-2018. https://www.epa.gov/ghgemissions/inventory-us-greenhouse-gas-emissions-and-sinks-1990-2018.

(2) Alvarez, R. A.; Zavala-Araiza, D.; Lyon, D. R.; Allen, D. T.; Barkley, Z. R.; Brandt, A. R.; Davis, K. J.; Herndon, S. C.; Jacob, D. J.; Karion, A.; Kort, E. A.; Lamb, B. K.; Lauvaux, T.; Maasakkers, J. D.; Marchese, A. J.; Omara, M.; Pacala, S. W.; Peischl, J.; Robinson, A. L.; Shepson, P. B.; Sweeney, C.; Townsend-Small, A.; Wofsy, S. C.; Hamburg, S. P. Assessment of Methane Emissions from the U.S. Oil and Gas Supply Chain. *Science* **2018**, *361*, 186−188.

(3) United State Environmental Protection Agency. 2014 National Emission Inventory (NEI) Report, https://www.epa.gov/sites/production/files/2016-12/documents/nei2014v1_tsd.pdf (accessed Mar 6, 2020).

(4) McKenzie, L. M.; Witter, R. Z.; Newman, L. S.; Adgate, J. L. Human Health Risk Assessment of Air Emissions from Development of Unconventional Natural Gas Resources. *Sci. Total Environ.* **2012**, *424*, 79−87.

(5) Adgate, J. L.; Goldstein, B. D.; McKenzie, L. M. Potential Public Health Hazards, Exposures and Health Effects from Unconventional Natural Gas Development. *Environ. Sci. Technol.* **2014**, *48*, 8307−8320.

(6) Tran, K. V.; Casey, J. A.; Cushing, L. J.; Morello-Frosch, R. Residential Proximity to Oil and Gas Development and Birth Outcomes in California: A Retrospective Cohort Study of 2006-2015 Births. *Environ. Health Perspect.* **2020**, *128*, No. 067001.

(7) Schnell, R. C.; Oltmans, S. J.; Neely, R. R.; Endres, M. S.; Molenar, J. V.; White, A. B. Rapid Photochemical Production of Ozone at High Concentrations in a Rural Site during Winter. *Nat. Geosci.* **2009**, *2*, 120−122.

(8) Han, C.; Liu, R.; Luo, H.; Li, G.; Ma, S.; Chen, J.; An, T. Pollution Profiles of Volatile Organic Compounds from Different Urban Functional Areas in Guangzhou China Based on GC/MS and PTR-TOF-MS: Atmospheric Environmental Implications. *Atmos. Environ.* **2019**, *214*, No. 116843.

(9) Luo, H.; Li, G.; Chen, J.; Lin, Q.; Ma, S.; Wang, Y.; An, T. Spatial and Temporal Distribution Characteristics and Ozone Formation Potentials of Volatile Organic Compounds from Three Typical Functional Areas in China. *Environ. Res.* **2020**, *183*, No. 109141.

(10) United States Environmental Protection Agency. Oil and Natural Gas Sector: Emission Standards for New, Reconstructed, and Modified Sources, https://www.govinfo.gov/content/pkg/FR-2016-06-03/pdf/2016-11971.pdf.

(11) United States Environmental; Protection Agency. Proposed Policy Amendments 2012 and 2016 New Source Performance Standards for the Oil and Natural Gas Industry, https://www.epa.gov/controlling-air-pollution-oil-and-natural-gas-industry/proposed-policy-amendments-2012-and-2016-new (accessed Mar 6, 2020).

(12) Warneke, C.; Geiger, F.; Edwards, P. M.; Dube, W.; Pétron, G.; Kofler, J.; Zahn, A.; Brown, S. S.; Graus, M.; Gilman, J. B.; Lerner, B. M.; Peischl, J.; Ryerson, T. B.; De Gouw, J. A.; Roberts, J. M. Volatile Organic Compound Emissions from the Oil and Natural Gas Industry in the Uintah Basin, Utah: Oil and Gas Well Pad Emissions Compared to Ambient Air Composition. *Atmos. Chem. Phys.* **2014**, *14*, 10977−10988.

(13) Edie, R.; Robertson, A. M.; Soltis, J.; Field, R. A.; Snare, D.; Burkhart, M. D.; Murphy, S. M. Off-Site Flux Estimates of Volatile Organic Compounds from Oil and Gas Production Facilities Using Fast-Response Instrumentation. *Environ. Sci. Technol.* **2020**, *54*, 1385−1394.

(14) Zavala-Araiza, D.; Alvarez, R. A.; Lyon, D. R.; Allen, D. T.; Marchese, A. J.; Zimmerle, D. J.; Hamburg, S. P. Super-Emitters in Natural Gas Infrastructure Are Caused by Abnormal Process Conditions. *Nat. Commun.* **2017**, *8*, No. 14012.

(15) Vaughn, T. L.; Bell, C. S.; Pickering, C. K.; Schwietzke, S.; Heath, G. A.; Pétron, G.; Zimmerle, D. J.; Schnell, R. C.; Nummedal, D. Temporal Variability Largely Explains Top-down/Bottom-up Difference in Methane Emission Estimates from a Natural Gas Production Region. *Proc. Natl. Acad. Sci. U.S.A.* **2018**, *115*, 11712−11717.

(16) Lavoie, T. N.; Shepson, P. B.; Cambaliza, M. O. L.; Stirm, B. H.; Conley, S.; Mehrotra, S.; Faloona, I. C.; Lyon, D. Spatiotemporal Variability of Methane Emissions at Oil and Natural Gas Operations in the Eagle Ford Basin. *Environ. Sci. Technol.* **2017**, *51*, 8001−8009.

(17) Duren, R. M.; Thorpe, A. K.; Foster, K. T.; Rafiq, T.; Hopkins, F. M.; Yadav, V.; Bue, B. D.; Thompson, D. R.; Conley, S.; Colombi, N. K.; Frankenberg, C.; McCubbin, I. B.; Eastwood, M. L.; Falk, M.; Herner, J. D.; Croes, B. E.; Green, R. O.; Miller, C. E. California's Methane Super-Emitters. *Nature* **2019**, *575*, 180−184.

(18) Karion, A.; Sweeney, C.; Pétron, G.; Frost, G.; Michael Hardesty, R.; Kofler, J.; Miller, B. R.; Newberger, T.; Wolter, S.; Banta, R.; Brewer, A.; Dlugokencky, E.; Lang, P.; Montzka, S. A.; Schnell, R.; Tans, P.; Trainer, M.; Zamora, R.; Conley, S. Methane Emissions Estimate from Airborne Measurements over a Western United States Natural Gas Field. *Geophys. Res. Lett.* **2013**, *40*, 4393−4397.

(19) Halliday, H. S.; Thompson, A. M.; Wisthaler, A.; Blake, D. R.; Hornbrook, R. S.; Mikoviny, T.; M??ller, M.; Eichler, P.; Apel, E. C.; Hills, A. J. Atmospheric Benzene Observations from Oil and Gas Production in the Denver-Julesburg Basin in July and August 2014. *J. Geophys. Res.: Atmos.* **2016**, *121*, 11,055−11,074.

(20) Müller, M.; Mikoviny, T.; Feil, S.; Haidacher, S.; Hanel, G.; Hartungen, E.; Jordan, A.; Märk, L.; Mutschlechner, P.; Schottkowsky, R.; Sulzer, P.; Crawford, J. H.; Wisthaler, A. A Compact PTR-ToF-MS Instrument for Airborne Measurements of Volatile Organic Compounds at High Spatiotemporal Resolution. *Atmos. Meas. Tech.* **2014**, *7*, 3763−3772.

(21) Zhou, X.; Aurell, J.; Mitchell, W.; Tabor, D.; Gullett, B. A Small, Lightweight Multipollutant Sensor System for Ground-Mobile and Aerial Emission Sampling from Open Area Sources. *Atmos. Environ.* **2017**, *154*, 31−41.

(22) Golston, L. M.; Tao, L.; Brosy, C.; Schäfer, K.; Wolf, B.; McSpiritt, J.; Buchholz, B.; Caulton, D. R.; Pan, D.; Zondlo, M. A.; Yoel, D.; Kunstmann, H.; McGregor, M. Lightweight Mid-Infrared Methane Sensor for Unmanned Aerial Systems. *Appl. Phys. B Lasers Opt.* **2017**, *123*, No. 170.

(23) Martinez, B.; Miller, T. W.; Yalin, A. P. Cavity Ring-down Methane Sensor for Small Unmanned Aerial Systems. *Sensors* **2020**, *20*, No. 454.

(24) Barchyn, T. E.; Hugenholtz, C. H.; Fox, T. A. Plume Detection Modeling of a Drone-Based Natural Gas Leak Detection System. *Elem. Sci. Anthropocene* **2019**, *7*, 41.
(25) United States Environmental Protection Agency. Method 21—Determination of Volatile Organic Compound Leak, https://www.epa.gov/sites/production/files/2017-08/documents/method_21.pdf.
(26) United States Environmental Protection Agency. Alternative Work Practice To Detect Leaks From Equipment. https://www.federalregister.gov/documents/2006/04/06/E6-5005/alternative-work-practice-to-detect-leaks-from-equipment (accessed Mar 6, 2020).
(27) Albertson, J. D.; Harvey, T.; Foderaro, G.; Zhu, P.; Zhou, X.; Ferrari, S.; Amin, M. S.; Modrak, M.; Brantley, H.; Thoma, E. D. A Mobile Sensing Approach for Regional Surveillance of Fugitive Methane Emissions in Oil and Gas Production. *Environ. Sci. Technol.* **2016**, *50*, 2487−2497.
(28) Brantley, H. L.; Thoma, E. D.; Squier, W. C.; Guven, B. B.; Lyon, D. Assessment of Methane Emissions from Oil and Gas Production Pads Using Mobile Measurements. *Environ. Sci. Technol.* **2014**, *48*, 14508−14515.
(29) Brantley, H. L.; Thoma, E. D.; Eisele, A. P. Assessment of Volatile Organic Compound and Hazardous Air Pollutant Emissions from Oil and Natural Gas Well Pads Using Mobile Remote and On-Site Direct Measurements. *J. Air Waste Manage. Assoc.* **2015**, *65*, 1072−1082.
(30) Warneke, C.; Veres, P.; Murphy, S. M.; Soltis, J.; Field, R. A.; Graus, M. G.; Koss, A.; Li, S. M.; Li, R.; Yuan, B.; Roberts, J. M.; De Gouw, J. A. PTR-QMS versus PTR-TOF Comparison in a Region with Oil and Natural Gas Extraction Industry in the Uintah Basin in 2013. *Atmos. Meas. Tech.* **2015**, *8*, 411−420.
(31) Zhou, X.; Passow, F. H.; Rudek, J.; Fisher, J. C. Von.; Hamburg, S. P.; Albertson, J. D. Estimation of Methane Emissions from the U. S. Ammonia Fertilizer Industry Using a Mobile Sensing Approach. *Elem. Sci. Anthropocene* **2019**, *7*, No. 19.
(32) Zhou, X.; Montazeri, A.; Albertson, J. D. Mobile Sensing of Point-Source Gas Emissions Using Bayesian Inference: An Empirical Examination of the Likelihood Function. *Atmos. Environ.* **2019**, *218*, No. 116981.
(33) Lavoie, T. N.; Shepson, P. B.; Cambaliza, M. O. L.; Stirm, B. H.; Conley, S.; Mehrotra, S.; Faloona, I. C.; Lyon, D. Spatiotemporal Variability of Methane Emissions at Oil and Natural Gas Operations in the Eagle Ford Basin. *Environ. Sci. Technol.* **2017**, *51*, 8001−8009.
(34) Roest, G.; Schade, G. Quantifying Alkane Emissions in the Eagle Ford Shale Using Boundary Layer Enhancement. *Atmos. Chem. Phys.* **2017**, *17*, 11163−11176.
(35) Peischl, J.; Eilerman, S. J.; Neuman, J. A.; Aikin, K. C.; de Gouw, J.; Gilman, J. B.; Herndon, S. C.; Nadkarni, R.; Trainer, M.; Warneke, C.; Ryerson, T. B. Quantifying Methane and Ethane Emissions to the Atmosphere From Central and Western U.S. Oil and Natural Gas Production Regions. *J. Geophys. Res.: Atmos.* **2018**, *123*, 7725−7740.
(36) Hildenbrand, Z.; Phillip, M.; McBride, E.; Navid Dorreyatim, M.; Taylor, J.; Carlton Jr, D.; Meik, J.; Fontenota, B.; Wrightg, K.; Schugae, K.; Verbeckc, G. Point Source Attribution of Ambient Contamination Events near Unconventional Oil and Gas Development. *Sci. Total Environ.* **2016**, *573*, 382−388.
(37) McHale, L. E.; Hecobian, A.; Yalin, A. P. Open-Path Cavity Ring-down Spectroscopy for Trace Gas Measurements in Ambient Air. *Opt. Express* **2016**, *24*, 5523.
(38) McHale, L. E.; Martinez, B.; Miller, T. W.; Yalin, A. P. Open-Path Cavity Ring-down Methane Sensor for Mobile Monitoring of Natural Gas Emissions. *Opt. Express* **2019**, *27*, 20084.
(39) Townsend-Small, A.; Marrero, J. E.; Lyon, D. R.; Simpson, I. J.; Meinardi, S.; Blake, D. R. Integrating Source Apportionment Tracers into a Bottom-up Inventory of Methane Emissions in the Barnett Shale Hydraulic Fracturing Region. *Environ. Sci. Technol.* **2015**, *49*, 8175−8182.
(40) Marrero, J. E.; Townsend-Small, A.; Lyon, D. R.; Tsai, T. R.; Meinardi, S.; Blake, D. R. Estimating Emissions of Toxic Hydrocarbons from Natural Gas Production Sites in the Barnett Shale Region of Northern Texas. *Environ. Sci. Technol.* **2016**, *50*, 10756−10764.
(41) Rella, C. W.; Tsai, T. R.; Botkin, C. G.; Crosson, E. R.; Steele, D. Measuring Emissions from Oil and Natural Gas Well Pads Using the Mobile Flux Plane Technique. *Environ. Sci. Technol.* **2015**, *49*, 4742−4748.
(42) Ion Science. Technical/Application Article 02, https://www.ionscience.com/wp-content/uploads/2017/03/TA-02-Ion-Science-PID-Response-Factors-UK-V1.14.pdf (accessed Aug 22, 2020).
(43) Zheng, H.; Kong, S.; Xing, X.; Mao, Y.; Hu, T.; DIng, Y.; Li, G.; Liu, D.; Li, S.; Qi, S. Monitoring of Volatile Organic Compounds (VOCs) from an Oil and Gas Station in Northwest China for 1 Year. *Atmos. Chem. Phys.* **2018**, *18*, 4567−4595.
(44) Ion Science. Ion Science. MiniPID 2 (3PIN) Instument User Manual V1.2, https://www.ionscience-usa.com/wp-content/uploads/2016/10/MiniPID-Manual-2-3-Pin-V1.2.pdf.
(45) United States Environmental Protection Agency. Method for the Determination of Volatile 697Organic Compounds in Ambient Air Using Cryogenic Preconcentration Techniques and 698Gas Chromatography with Flame Ionization and Electron Capture Detection, https://www.epa.gov/sites/production/files/2019-11/documents/to-3.pdf.
(46) Marrero, J. E.; Townsend-Small, A.; Lyon, D. R.; Tsai, T. R.; Meinardi, S.; Blake, D. R. Estimating Emissions of Toxic Hydrocarbons from Natural Gas Production Sites in the Barnett Shale Region of Northern Texas. *Environ. Sci. Technol.* **2016**, *50*, 10756−10764.
(47) Zhou, X.; Yoon, S.; Mara, S.; Falk, M.; Kuwayama, T.; Tran, T.; Cheadle, L.; Nyarady, J.; Croes, B.; Scheehle, E.; Herner, J. D.; Vijayan, A. Mobile Sampling of Methane Emissions from Natural Gas Well Pads in California. *Atmos. Environ.* **2021**, *244*, No. 117930.
(48) Belušíc, D.; H Lenschow, D.; Tapper, N. J. Performance of a Mobile Car Platform for Mean Wind and Turbulence Measurements. *Atmos. Meas. Tech.* **2014**, *7*, 1825−1837.
(49) Yee, E. Bayesian Probabilistic Approach for Inverse Source Determination from Limited and Noisy Chemical or Biological Sensor Concentration Measurements, *Proceedings of SPIE*, 2007, 6554 (November), 65540W.
(50) Gryning, S.; Ulden, A. P.; van Larsen, S. E. Dispersion from a Continuous Ground-Level Source Investigated by a K Model. *Q. J. R. Meteorol. Soc.* **1983**, *109*, 355−364.
(51) Bell, C.; Vaughn, T.; Zimmerle, D. Evaluation of next Generation Emission Measurement Technologies under Repeatable Test Protocols. *Elem. Sci. Anth.* **2020**, *8*, 32.
(52) Gvakharia, A.; Kort, E. A.; Smith, M. L.; Conley, S. Evaluating Cropland N2O Emissions and Fertilizer Plant Greenhouse Gas Emissions With Airborne Observations. *J. Geophys. Res.: Atmos.* **2020**, *125*, No. e2020JD032815.
(53) Texas Commission on Environmental Quality. Karnes County [36] Monthly Summary. https://www.tceq.texas.gov/cgi-bin/compliance/monops/agc_monthly_summary.pl.
(54) Mooney, C. F.; Mooney, C. L.; Mooney, C. Z.; Duval, R. D.; Duvall, R. *Bootstrapping: A Nonparametric Approach to Statistical Inference*; Sage, 1993.
(55) Omara, M.; Zimmerman, N.; Sullivan, M. R.; Li, X.; Ellis, A.; Cesa, R.; Subramanian, R.; Presto, A. A.; Robinson, A. L. Methane Emissions from Natural Gas Production Sites in the United States: Data Synthesis and National Estimate. *Environ. Sci. Technol.* **2018**, *52*, 12915−12925.
(56) Gidney, B.; Pena, S. Upstream Oil and Gas Storage Tank Project Flash Emissions Models Evaluation, https://www.tceq.texas.gov/assets/public/implementation/air/am/contracts/reports/ei/20090716-ergi-UpstreamOilGasTankEIModels.pdf. (accessed Mar 6, 2020).
(57) Zavala-Araiza, D.; Lyon, D. R.; Alvarez, R. A.; Davis, K. J.; Harriss, R.; Herndon, S. C.; Karion, A.; Kort, E. A.; Lamb, B. K.; Lan, X.; Marchese, A. J.; Pacala, S. W.; Robinson, A. L.; Shepson, P. B.; Sweeney, C.; Talbot, R.; Townsend-Small, A.; Yacovitch, T. I.; Zimmerle, D. J.; Hamburg, S. P. Reconciling Divergent Estimates of Oil and Gas Methane Emissions. *Proc. Natl. Acad. Sci.* **2015**, *112*, 15597−15602.
(58) Omara, M.; Sullivan, M. R.; Li, X.; Subramian, R.; Robinson, A. L.; Presto, A. A. Methane Emissions from Conventional and

https://dx.doi.org/10.1021/acs.est.0c06545
Environ. Sci. Technol. 2021, 55, 581−592

Unconventional Natural Gas Production Sites in the Marcellus Shale Basin. *Environ. Sci. Technol.* **2016**, *50*, 2099−2107.
(59) United States Environmental Protection Agency. Nonhalogenated Organics by Gas Chromatography, https://www.epa.gov/hw-sw846/sw-846-test-method-8015c-nonhalogenated-organics-gas-chromatography.
(60) Allen, D.; Torres, V.; Thomas, J.; Sullivan, D.; et al. Measurements of Methane Emissions at Natural Gas Production Sites in the United States. *Proc. Natl. Acad. Sci. U.S.A.* **2013**, *110*, 17768−17773.

https://dx.doi.org/10.1021/acs.est.0c06545
Environ. Sci. Technol. 2021, 55, 581−592